View Online / Journal Homepage / Table of Contents for this issue
Dynamic Article Links

Journal of Materials Chemistry

Cite this: *J. Mater. Chem.*, 2012, **22**, 6307

www.rsc.org/materials

PAPER

Large-area, highly oriented lamellar block copolymer nanopatterning directed by graphoepitaxially assembled cylinder nanopatterns†

Hyoung-Seok Moon,[a] Dong Ok Shin,[a] Bong Hoon Kim,[a] Hyeong Min Jin,[a] Sumi Lee,[b] Moon Gyu Lee[b] and Sang Ouk Kim*[a]

Received 14th November 2011, Accepted 19th January 2012
DOI: 10.1039/c2jm15842f

Downloaded by Korea Advanced Institute of Science & Technology / KAIST on 30 April 2012
Published on 21 February 2012 on http://pubs.rsc.org | doi:10.1039/C2JM15842F

We present a large-area, highly aligned lamellar block copolymer self-assembly directed by graphoepitaxially aligned cylinder block copolymer self-assembly. Asymmetric block copolymer thin films were graphoepitaxially assembled within 1 μm wide parallel photoresist trenches to generate surface-parallel nanocylinder arrays. After the graphoepitaxial morphology was frozen by a radiative treatment, a thin film of symmetric block copolymer was deposited over the nanocylinder array, where the lamellar period was consistent with the period of the underlying cylinder array. Subsequent thermal annealing generated highly aligned lamellar morphology over a large area without any trace of an underlying photoresist pattern. Our method employing surface-parallel cylinder self-assembly as a structure-directing chemical pattern for epitaxial self-assembly does not require any substrate surface pretreatment and is, thus, highly efficient for nanopatterning various substrates.

Introduction

Block copolymer lithography exploits the self-assembled nanoscale morphologies of block copolymer thin films for low-cost, high-throughput production of dense nanopatterns over an arbitrary large area.[1–4] To date, block copolymer lithography has become a strong candidate to complement the intrinsic resolution limitation of conventional optical lithography. Nevertheless, the successful establishment of ultimate block copolymer lithography requires the directed self-assembly of highly ordered nanopatterns with minimized pattern imperfections.[5–28] To this end, numerous approaches have been explored thus far, including the application of external field[4,20,24,27,28] and epitaxial assembly on chemically/topographically prepatterned substrates.[5–9,11–13,15,18,23,26]

In this contribution, we present a block copolymer lithography integrated with conventional I-line photolithography for highly ordered lamellar nanopatterns over an arbitrary large area. I-line lithography employing a 365 nm wavelength ultraviolet (UV) light source is widely used for micrometre scale photoresist patterning. We employed this conventional photolithography to prepare 1 μm scale line/space patterns of a negative tone photoresist upon an arbitrary substrate. A single layer cylinder forming block copolymer thin film was deposited within the trenches of the photoresist pattern. Subsequent thermal annealing induced the graphoepitaxial assembly of substrate parallel cylinders along the photoresist trench walls. This graphoepitaxy morphology composed of highly aligned nanocylinders and photoresist mesas was utilized as the chemical prepattern to direct the highly ordered lamellar pattern. A lamellar block copolymer film, whose lamellar period is commensurate with that of the underlying cylinder pattern, was spin cast onto the graphoepitaxy pattern and thermally annealed to form highly aligned lamellae. While the lamellar arrays on the cylinder pattern were registered by the surface energy modulation of the underlying cylinder pattern, the lamellar arrays on the photoresist mesa were forced to align by the neighboring highly aligned lamellae. As a consequence, this approach successfully transformed a micrometre scale I-line photolithography pattern into a sub-30 nm scale lamellar pattern *via* all parallel processing. In addition, since the surface-parallel cylinder pattern was used as a chemical pattern, this approach can be generally utilized for various substrate materials without any surface modification for surface-perpendicular nanodomain alignment.

[a]*Department of Materials Science and Engineering, KAIST, Daejeon, 305-701, Republic of Korea. E-mail: sangouk.kim@kaist.ac.kr; Fax: +82 42 350 3310; Tel: +82 42 350 3339*
[b]*LCD R&D Center, Samsung Electronics, 446-920 446-711 95 Samsung2-Ro, Kihung-Gu, Yong-In City, Kyungki-Do, 446-920, Korea*
† Electronic supplementary information (ESI) available. See DOI: 10.1039/c2jm15842f

Experimental

Photoresist confinement preparation

A 100 nm thick photoresist layer (SU8, MicroChem Corp. US) was spin-cast onto a silicon substrate and soft baked at 95 °C for 60 s to evaporate residual solvent and densify the film. The photoresist film was exposed to an I-line source (Midas/MDA-6000 DUV, KR; wavelength: 365 nm; 9.5 mW cm^{-2}) through a photomask and post baked at 110 °C for 95 s to selectively crosslink the exposed portions of the photoresist film. The

pattern development was performed by immersing the exposed photoresist film into a propylene glycol methyl ether acetate (PGMEA) solution for 60 s.[18,22,23,25] After the pattern development, the thickness of the patterned photoresist was decreased to a desired value by dry-etching with O_2 plasma.

Directed self-assembly of PS-*b*-PMMA thin films

Thin films of an asymmetric polystyrene-*block*-poly(methyl methacrylate) (PS-*b*-PMMA) diblock copolymer having the number average molecular weights (M_n) of 46 kg mol^{-1} and 21 kg mol^{-1} or 140 kg mol^{-1} and 60 kg mol^{-1} for PS and PMMA blocks, respectively, were spin-cast from a toluene solution over the photopatterned surface. Thermal annealing was conducted at 250 °C for the directed self-assembly into equilibrium morphology. The resultant graphoepitaxially assembled morphology consisting of parallel cylinder arrays highly aligned along parallel photoresist trenches was crosslinked by a brief UV irradiation ($\lambda = 255$ nm). After the chemical freezing of block copolymer films, thin films of symmetric PS-*b*-PMMA block copolymer blends (3 : 7 blends of PS-*b*-PMMA1 (M_n: 50 kg mol^{-1}) and PS-*b*-PMMA2 (M_n: 72 kg mol^{-1}) or 83 : 27 blends of PS-*b*-PMMA3 (M_n: 160 kg mol^{-1}) and PS-*b*-PMMA4 (M_n: 10 kg mol^{-1})) were spin cast from a toluene solution onto the entire substrate. Subsequent thermal annealing for directed self-assembly was conducted at 280 °C for several hours.

TiO_2 and Au deposited substrate preparation

TiO_2 thin film was deposited by the atomic layer deposition (ALD) process.[14] Au thin film was deposited by thermal evaporation.[22] The thicknesses of TiO_2 and Au were 40 and 100 nm, respectively.

Characterization

The nanoscale morphology of the block copolymer thin film was imaged using a Hitachi S-4800 SEM with a field emission source at 1 kV.

Results and discussion

The overall nanolithography process is schematically described in Fig. 1. Firstly, a negative tone photoresist (SU8) was uniformly spin-cast onto a substrate and topographically patterned by conventional I-line photolithography (I-line source; wavelength 365 nm; 9.5 mW cm^{-2}). We used bare silicon substrates without any surface modification. This base silicon substrate showed strong polar characteristics due to the oxygen functional groups present at native silicon oxide surfaces. A thin film of asymmetric PS-*b*-PMMA copolymer, with a hexagonal cylinder self-assembled morphology, was spin cast onto the topographic pattern of the photoresist and annealed at a high temperature for directed assembly into a highly ordered parallel PS-*b*-PMMA cylinder array. After thermal treatment, the cylinder PS-*b*-PMMA pattern was briefly exposed to UV radiation to selectively crosslink the PS block. This radiative treatment prevented any damage to the self-assembled block copolymer thin films during the subsequent solution casting of the lamellar block copolymer film. Finally, a thick film of PS-*b*-PMMA, forming the lamellar phase, was spin cast onto the cylinder PS-*b*-PMMA chemical pattern and thermally annealed for a large-area lamellar nanopattern.

Fig. 2A and B show the cylinder-forming block copolymer thin films self-assembled within the topographic confinement from parallel photoresist trenches. Highly aligned, monolayered, surface-parallel nanoscale cylinders were assembled along photoresist trenches that were ~1 μm wide. The asymmetric PS-*b*-PMMA block copolymer used for Fig. 2A had a M_n of 46 kg mol^{-1} for the PS block and 21 kg mol^{-1} for the PMMA block, respectively, with a natural cylinder layer period (l_0) of 42 nm.

In contrast, a M_n of the block copolymer used for Fig. 2B was 140 kg mol^{-1} for the PS block and 60 kg mol^{-1} for the PMMA

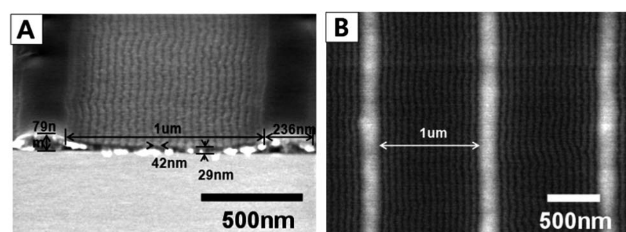

Fig. 2 SEM images of graphoepitaxial nanocylinder arrays. (a) Cross-sectional SEM image of a graphoepitaxially assembled nanocylinder array within a 1 μm photoresist trench. (b) Plane view of highly aligned nanocylinder arrays within a 1 μm photoresist trench.

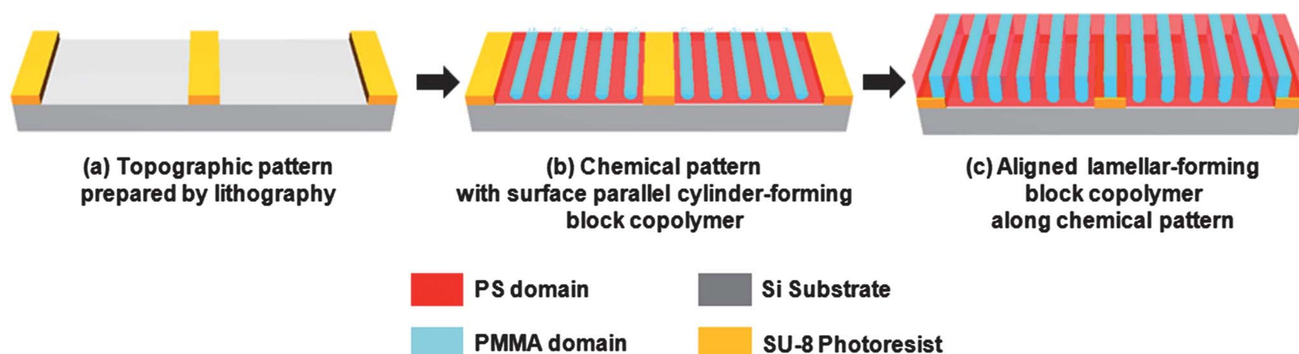

Fig. 1 Schematic procedure for highly aligned lamellar block copolymer nanopattern. (a) Topographic photoresist patterning by I-line lithography. (b) Graphoepitaxial assembly of monolayered block copolymer cylinder array. (c) Highly oriented block copolymer lamellar pattern directed by underlying graphoepitaxial morphology.

Downloaded by Korea Advanced Institute of Science & Technology / KAIST on 30 April 2012
Published on 21 February 2012 on http://pubs.rsc.org | doi:10.1039/C2JM15842F

This journal is © The Royal Society of Chemistry 2012

Published on 21 February 2012 on http://pubs.rsc.org | doi:10.1039/C2JM15842F
Downloaded by Korea Advanced Institute of Science & Technology / KAIST on 30 April 2012

block, respectively, with a l_0 of 64 nm. Thermal annealing was performed at 280 °C for 3 h under an inert N_2 atmosphere.

The block copolymer film with a highly aligned self-assembled cylinder array could be frozen by UV crosslinking, as shown in Fig. 3. The UV radiation ($\lambda = 255$ nm) used in this work selectively crosslinked the PS block. Since it degraded the PMMA block, the radiation dose was precisely controlled to minimize the degradation effect. When the dose of UV radiation was insufficient (Fig. 3A–C), the top layer of lamellar PS-*b*-PMMA showed a hole and island morphology. An insufficiently crosslinked bottom block copolymer layer was damaged or washed away during the spin casting of the top layer to reveal a bare silicon substrate. The preferential absorption of the PMMA component at the bare silicon surface generated surface-parallel lamellae, which resulted in the hole and island morphology with the quantized film thickness. Meanwhile, when the UV dose was 4 J cm^{-2}, the top lamellar block copolymer layer showed a surface-perpendicular lamellar morphology. This morphology was epitaxially registered by the underlying frozen surface-parallel cylinder array. We note that our approach employing surface-parallel cylinder self-assembly as a structure-directing chemical pattern requires no chemical substrate pretreatment, such as polymer brush layer formation or self-assembled monolayer deposition. Therefore, this approach is highly efficient for the nanopatterning of arbitrary substrates with different surface energy levels. We demonstrate this versatility by the control experiments using TiO_2 and Au substrates. While self-assembled lamellae on bare TiO_2 or Au substrate aligned in the surface parallel direction, those formed on the substrates covered with monolayered surface-parallel cylinder self-assembly showed surface perpendicular orientation (Fig. S1†).

For an optimized registration of the lamellar pattern by the underlying cylinder pattern, the commensurability of the pattern period was crucial. It has been reported that a slight mismatch of the pattern periods results in poorly aligned morphologies with many defects, such as dislocation pairs or tilted, undulated lamellae.[29] The lamellar period of the top film layer could be

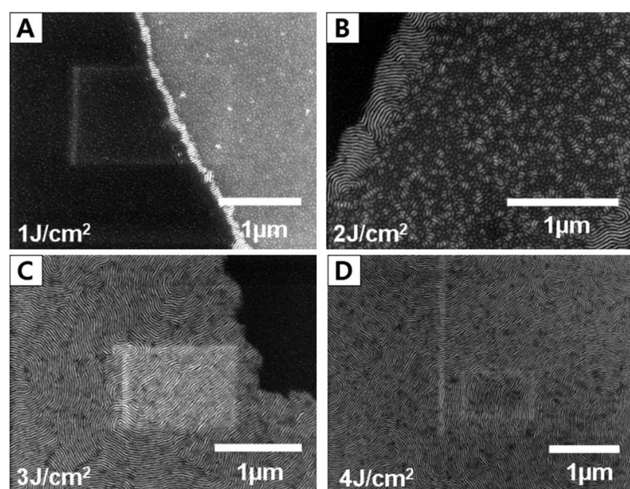

Fig. 3 SEM images of lamellar block copolymer films assembled on a surface-parallel cylinder pattern frozen by UV crosslinking ($\lambda = 255$ nm). The UV doses were (a) 1 J cm^{-2}, (b) 2 J cm^{-2}, (c) 3 J cm^{-2}, and (d) 4 J cm^{-2}, respectively.

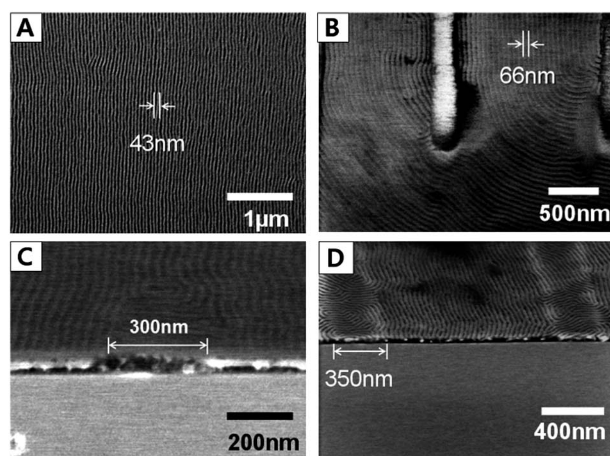

Fig. 4 SEM images of highly oriented block copolymer lamellar patterns assembled on block copolymer nanocylinder arrays. (a) Highly aligned lamellae of 3 : 7 blends of PS-*b*-PMMA1 (M_n: 50 kg mol^{-1}) and PS-*b*-PMMA2 (M_n: 72 kg mol^{-1}) without any trace of an underlying photoresist pattern and (b) highly aligned lamellae of 83 : 27 blends of PS-*b*-PMMA3 (M_n: 160 kg mol^{-1}) and PS-*b*-PMMA4 (M_n: 10 kg mol^{-1}) at the edge of the photoresist pattern. Lamellar morphology on photoresist mesas of (c) 300 nm and (d) 350 nm width, respectively.

precisely controlled by blending two lamellar block copolymers.[13] Various block copolymer blends, including 3 : 7 blends of PS-*b*-PMMA1 (M_n: 50 kg mol^{-1}) and PS-*b*-PMMA2 (M_n: 72 kg mol^{-1}) with a l_0 of 43 nm (Fig. 4A) and 83 : 27 blends of PS-*b*-PMMA3 (M_n: 160 kg mol^{-1}) and PS-*b*-PMMA4 (M_n: 10 kg mol^{-1}) with a l_0 of 66 nm (Fig. 4B), were deposited and thermally annealed. As shown in Fig. 4A and B, highly aligned lamellar patterns epitaxially registered by underlying cylinder patterns were attainable if the pattern periods were commensurate.

In the photoresist mesa region, there is no chemical modulation to direct lamellar block copolymer assembly. However, when the photoresist mesa width was sufficiently narrow below 300 nm, the lamellar arrays on the photoresist mesa were forced to align along the neighboring highly aligned lamellae to form surface-perpendicular lamellar arrays, as shown in Fig. 4C. The resultant morphology showed a highly aligned lamellar array over an arbitrary large area without any trace of a structure directing photoresist pattern at the top lamellar film surface. In contrast, when the photoresist mesa width was larger than 300 nm, the enforced alignment of lamellae could not cross over the entire mesa width. As a result, the lamellar alignment on the photoresist mesa region showed random orientated lamellae with a high density of defects, which clearly contrasts with the highly aligned lamellar film in the neighboring photoresist trench region (Fig. 4D).

Conclusions

We achieved arbitrary large-area directed self-assembly of 20 nm scale block copolymer lamellar patterns from conventional I-line lithography. A highly oriented nanoscale cylinder array was graphoepitaxially assembled within 1 μm width photoresist trenches prepared by I-line lithography. The subsequent spin casting of the lamellar block copolymer film and thermal annealing over the graphoepitaxy morphology attained a highly

Downloaded by Korea Advanced Institute of Science & Technology / KAIST on 30 April 2012
Published on 21 February 2012 on http://pubs.rsc.org | doi:10.1039/C2JM15842F

aligned surface-perpendicular lamellar pattern epitaxially registered by the underlying cylinder pattern. It is noteworthy that the self-assembled lamellae formed on the photoresist mesa were also highly aligned along the neighbouring lamellae epitaxially registered by the underlying cylinder pattern. The resultant self-assembled lamellar film showed a highly aligned large-area lamellar pattern with no trace of a photoresist pattern. Overall, this block copolymer lithography integrated with I-line lithography successfully transformed a micrometre scale I-line photopattern into a sub-30 nm scale lamellar pattern *via* all parallel processing. Furthermore, this process, employing a surface-parallel cylinder array as a chemical pattern to direct overlay self-assembly, offered a high-aspect-ratio surface-perpendicular lamellar pattern on various substrates without any neutral surface modification for perpendicular nanodomain alignment.

Acknowledgements

This work was supported by LCD R&D Center, Samsung Electronics, National Research Laboratory Program (R0A-2008-000-20057-0), Platform Project grant (10033636-2009-11) and the Smart IT Convergence System Research Center (Global Frontier Project, SIRC-2011-0031852) funded by the Korean government (MEST, MKE).

Notes and references

1 F. S. Bates and G. H. Fredrickson, *Phys. Today*, 1999, **52**, 32.
2 C. J. Hawker and T. P. Russell, *MRS Bull.*, 2005, **30**, 952.
3 M. Park, C. Harrison, P. M. Chaikin, R. A. Register and D. H. Adamson, *Science*, 1997, **276**, 1401.
4 T. Thurn-Albrecht, J. Schotter, G. A. Kästle, N. Emley, T. Shibauchi, L. Krusin-Elbaum, K. Guarini, C. T. Black, M. T. Tuominen and T. P. Russell, *Science*, 2000, **290**, 2126.
5 R. A. Segalman, H. Yokoyama and E. J. Kramer, *Adv. Mater.*, 2001, **13**, 1152.
6 S. O. Kim, H. H. Solak, M. P. Stoykovich, M. J. Ferrier, J. J. de Pablo and P. F. Nealey, *Nature*, 2002, **424**, 411.
7 D. Sundrani, S. B. Darlling and S. J. Sibener, *Nano Lett.*, 2004, **4**, 273.
8 J. Y. Cheng, A. M. Mayes and C. A. Ross, *Nat. Mater.*, 2004, **3**, 823.
9 M. P. Stoykovich, M. Muller, S. O. Kim, H. H. Solak, E. W. Edwards, J. J. de Pablo and P. F. Nealey, *Science*, 2005, **308**, 1442.
10 D. Y. Ryu, K. Shin, E. Drockenmuller, C. J. Hawker and T. P. Russell, *Science*, 2005, **308**, 236.
11 S. O. Kim, B. H. Kim, D. Meng, D. O. Shin, C. M. Koo, H. H. Solak and Q. Wang, *Adv. Mater.*, 2007, **19**, 3271.
12 Y. S. Jung, W. Jung, H. L. Tuller and C. A. Ross, *Nano Lett.*, 2007, **8**, 3776.
13 R. Ruiz, R. L. Sandstrom and C. T. Black, *Adv. Mater.*, 2007, **19**, 587.
14 S.-J. Jeong, G. Xia, B. H. Kim, D. O. Shin, S.-H. Kwon, S.-W. Kang and S. O. Kim, *Adv. Mater.*, 2008, **20**, 1898.
15 R. Ruiz, H. Kang, F. A. Detcheverry, E. Dobisz, D. S. Kercher, T. R. Albrecht, J. J. de Pablo and P. F. Nealey, *Science*, 2008, **321**, 936.
16 C. T. Black, R. Ruiz, G. Breyta, J. Y. Cheng, M. E. Colburn, K. W. Guarini, H.-C. Kim and Y. Zhang, *IBM J. Res. Dev.*, 2007, **51**, 605.
17 C. Tang, E. M. Lennon, G. H. Fredrickson, E. J. Kramer and C. J. Hawker, *Science*, 2008, **322**, 429.
18 S.-J. Jeong, J. E. Kim, H.-S. Moon, B. H. Kim, S. M. Kim, J.-B. Kim and S. O. Kim, *Nano Lett.*, 2009, **9**, 2300.
19 D. O. Shin, B. H. Kim, J. H. Kang, S.-J. Jeong, S. H. Park, Y.-H. Lee and S. O. Kim, *Macromolecules*, 2009, **42**, 1189.
20 B. H. Kim, H. M. Lee, J.-H. Lee, S.-W. Son, S.-J. Jeong, S. M. Lee, D. I. Lee, S. W. Kwak, H. W. Jeong, H. J. Shin, J.-B. Yoon, O. D. Lavrentovich and S. O. Kim, *Adv. Funct. Mater.*, 2009, **19**, 2584.
21 D. O. Shin, J. R. Jeong, T. H. Han, C. M. Koo, H. J. Park, Y. T. Lim and S. O. Kim, *J. Mater. Chem.*, 2010, **20**, 7241.
22 S.-J. Jeong, H.-S. Moon, J.-H. Shin, B.-H. Kim, D. O. Shin, J. Y. Kim, Y. H. Lee, J. U. Kim and S. O. Kim, *Nano Lett.*, 2010, **10**, 3500.
23 S.-J. Jeong, H.-S. Moon, B. H. Kim, D. O. Shin, J. Y. Kim, J. Yu, S. Lee, M. G. Lee, H. Y. Cho and S. O. Kim, *ACS Nano*, 2010, **4**, 5181.
24 B. H. Kim, J. Y. Kim, S.-J. Jeong, J. O. Hwang, D. H. Lee, D. O. Shin, S. Y. Choi and S. O. Kim, *ACS Nano*, 2010, **4**, 5464.
25 S.-J. Jeong and S. O. Kim, *J. Mater. Chem.*, 2011, **21**, 5856.
26 H. Jung, D. Hwang, E. Kim, B.-J. Kim, W. B. Lee, J. E. Poelma, J. Kim, C. J. Hawker, J. Huh, D. Y. Ryu and J. Bang, *ACS Nano*, 2011, **5**, 6164.
27 M. Cavallini, J. Gomez-Segura, C. Albonetti, D. Ruiz-Molina, J. Veciana and F. Biscarini, *J. Phys. Chem. B*, 2006, **110**, 11607.
28 M. Cavallini, *J. Mater. Chem.*, 2009, **19**, 6085.
29 S. O. Kim, B. H. Kim, K. Kim, C. M. Koo, M. P. Stoykovich, P. F. Nealey and H. H. Solak, *Macromolecules*, 2006, **39**, 5466.

 This journal is © The Royal Society of Chemistry 2012